APPENDIX

"Centriolar distal appendages activate the centrosome-PIDDosome-p53 signaling axis via ANKRD26"

Matteo Burigotto, Alessia Mattivi, Daniele Migliorati, Giovanni Magnani, Chiara Valentini, Michela Roccuzzo, Martin Offterdinger, Massimo Pizzato, Alexander Schmidt, Andreas Villunger, Stefano Maffini, and Luca L. Fava

Table of Contents

A)

Clone Name	Cell line	gRNA sequence	Type of INDEL	ICE KO score	Immunoblot characterization	MDM2 cleavage proficiency
CEP83 3#4	A549	AAGAATACAGGTGCGGCAGT	+1	99	Yes (App. Fig. S1B)	No
CEP83 4#2	A549	GGCTGAAGTAGCGGAATTAA	-344	n.a.	Yes (App. Fig. S1B)	No
CEP83 3#A3	RPE1	AAGAATACAGGTGCGGCAGT	-7, -11	94	Yes (App. Fig. S1B)	No
CEP83 3#A5	RPE1	AAGAATACAGGTGCGGCAGT	-7	99	Yes (App. Fig. S1B)	No
SCLT1 2#D1	A549	GGGCCTCAGTCATATGTTCC	-2, -8	97	n.a.	No
SCLT1 2#1	RPE1	GGGCCTCAGTCATATGTTCC	+1	99	n.a.	No
ANKRD26 2#22	A549	GCTCCTCTGCCGCCGCGCGA	-7, -2	94	Yes (Fig. 5A)	No
ANKRD26 4#28	RPE1	ATGTCTGTGACAACGAAAAC	+1	99	Yes (Fig. 3F)	No
PIDD1 2#10	A549	GCCGATAGCGGATGGTGATG	+1	99	n.a.	No
PIDD1 2#5	RPE1	GCCGATAGCGGATGGTGATG	n.a.	n.a.	n.a.	No
PIDD1 4#10	RPE1	GGCCCGGCGCTGCCGTGAAG	-10	99	n.a.	No
FBF1 1#3	RPE1	TATCAGCATCCATGCCGTCC	+1	99	n.a.	Yes
CEP164 2#25	RPE1	CTGATGTGGCTGGCGCGAGA	-2	100	n.a.	Yes
TP53 4#1	A549	TCCATTGCTTGGGACGGCAA	-218	n.a.	Yes (App. Fig. S1E)	n.a.
TP53 4#9	RPE1	TCCATTGCTTGGGACGGCAA	-725	n.a.	Yes (App. Fig. S1E)	n.a.

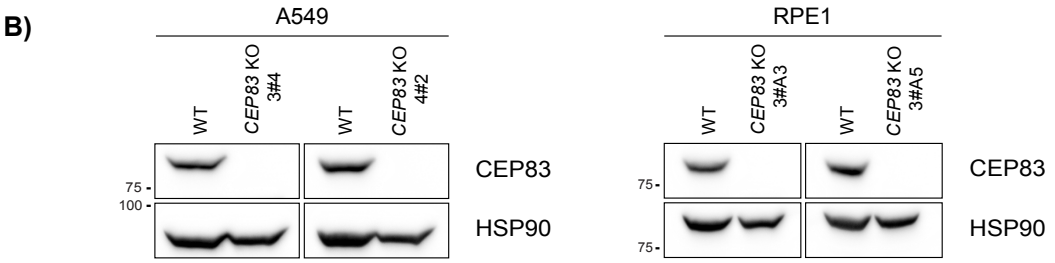

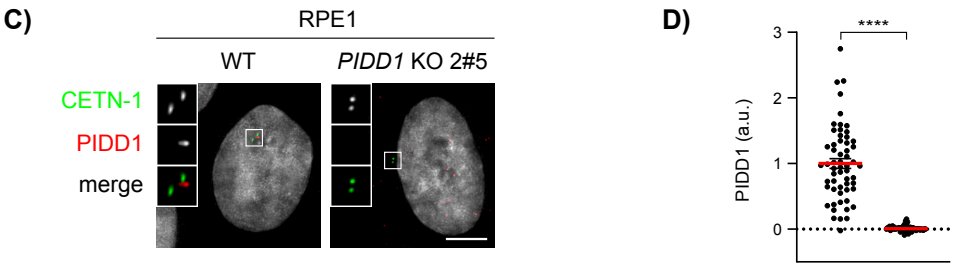

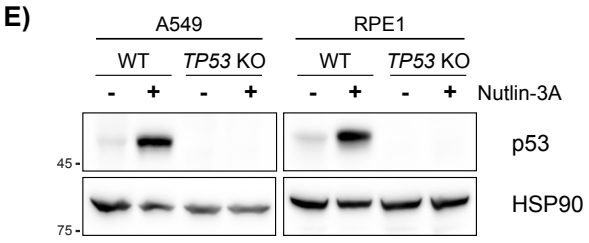

Appendix Figure S1. Characterization of knock-out cell lines generated in this study. (A) Comprehensive list of CRISPR/Cas9 knock-out clones used in this study and their molecular/functional characterization; n.a. = not applicable. **(B)** A549 and RPE1 cells of the indicated genotype were subjected to immunoblot. **(C)** Representative immunofluorescence micrograph from the indicated cell lines co-stained with the indicated antibodies. Blow-ups without Hoechst 33342 are magnified 2.5X. Scale bar: 5 μm. **(D)** Dot plot showing the PIDD1 average pixel intensity at individual centrioles. Data obtained from images as in (C). N ≥ 50 centrosomes were assessed for each condition in as many individual cells, a.u. = arbitrary units. Mann-Whitney test. **(E)** A549 and RPE1 cell lines of the indicated genotypes were either left untreated or treated with 10 μM Nultin-3a for 24h and subjected to immunoblot.

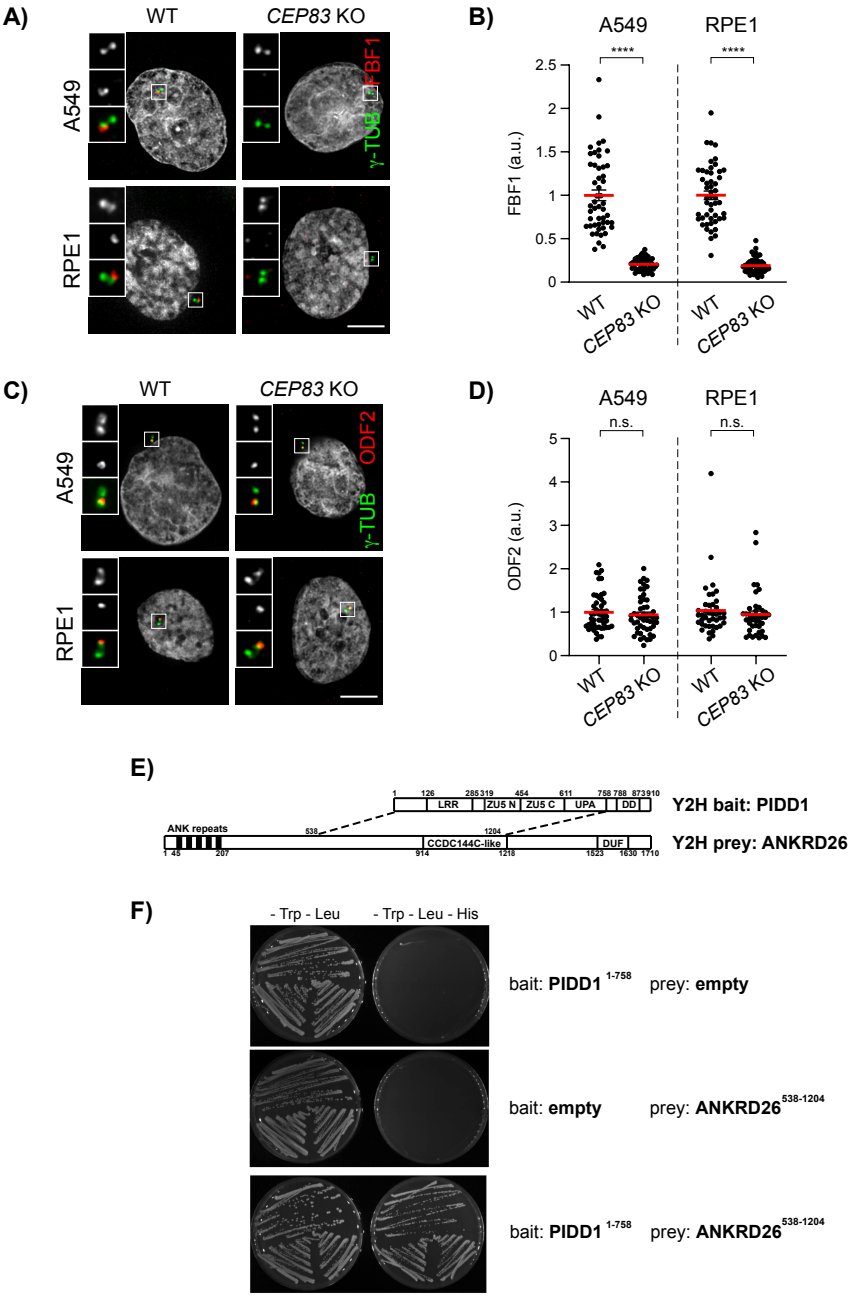

Appendix Figure S2. Characterization of appendage-deficient cell lines and PIDD1:ANKRD26 yeast-two-hybrid interaction. (A) Representative fluorescence micrographs from the indicated cell lines co-stained with the indicated antibodies. Blow-ups without Hoechst 33342 are magnified 2.5X. Scale bar: 5 µm. **(B)** Dot plots showing the FBF1 average pixel intensities at individual parental centrioles. Data obtained from images as in (A). N ≥ 50 centrosomes were assessed for each condition in as many individual cells, a.u. = arbitrary units. Mann-Whitney test. **(C)** Representative fluorescence micrographs from the indicated cell lines co-stained with the indicated antibodies. Blow-ups without Hoechst 33342 are magnified 2.5X. Scale bar: 5 µm. **(D)** Dot plots showing the FBF1 average pixel intensities at individual parental centrioles. Data obtained from images as in (A). N ≥ 50 centrosomes were assessed for each condition in as many individual cells, a.u. = arbitrary units. Mann-Whitney test. **(E)** Schematic of the domain structures of PIDD1 and ANKRD26. The bait utilized in the screen corresponded to PIDD1$^{S446A-S588A}$ a.a. 1-758 and retrieved as prey the 538-1204 fragment of ANKRD26. ANKRD26 annotated domains: ANK repeats = Ankyrin repeats, CCDC144C-like = Coiled-coil domain similar to CCDC144C, DUF: Domain of Unknown Function. For PIDD1 domain descriptions see Fig. 4A. **(F)** One by one interaction between the PIDD1 bait and the ANKRD26 prey plasmid isolated from the screen. Yeasts transformed with the indicated bait and prey plasmids were tested for growth on selective plates devoid of tryptophan and leucine (-Trp -Leu) or devoid of tryptophan, leucine and histidine (-Trp -Leu - His).

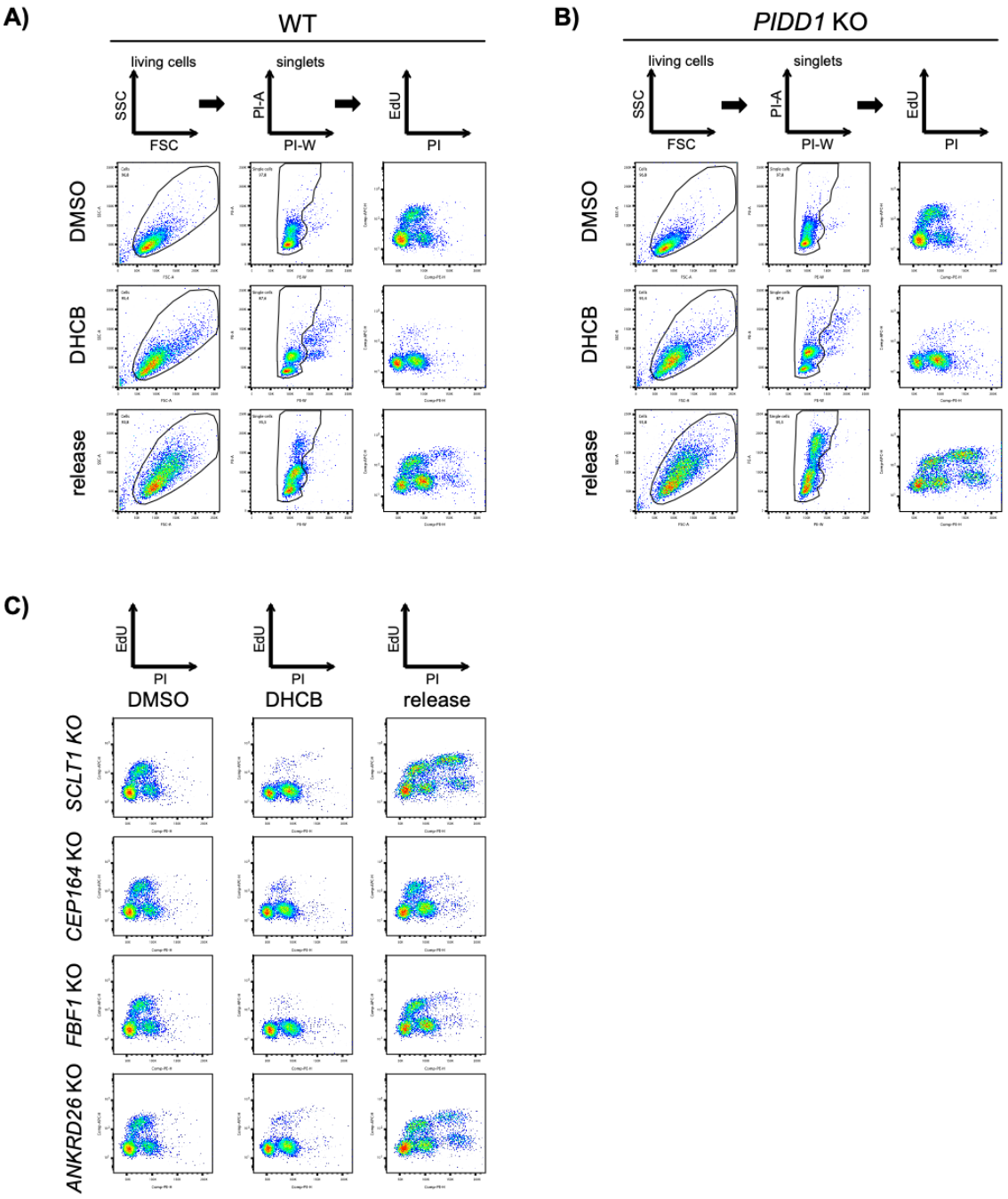

Appendix Figure S3. Representative raw data and gating strategies relative to Fig. 3E (A-B) Chosen gating strategy for the assessment of genome reduplication upon cytokinesis failure, displayed for RPE1 parental cells (A), showing a limited degree of genome duplication, as well as for *PIDD1* KO RPE1 derivatives (B), showing a high degree of genome reduplication. RPE1 cells of the indicated genotypes were treated either with DMSO or with DHCB for 24h. A fraction of DHCB treated cells were released into fresh medium for other 24h (release), allowing to assess the degree of genome reduplication. FSC = forward scatter, SSC = side scatter, PI = propidium iodide, EdU = 5-Ethynyl-2´-deoxyuridine. **(C)** PI vs EdU dot plots of the indicated RPE1 genotypes treated and gated as in (A-B).

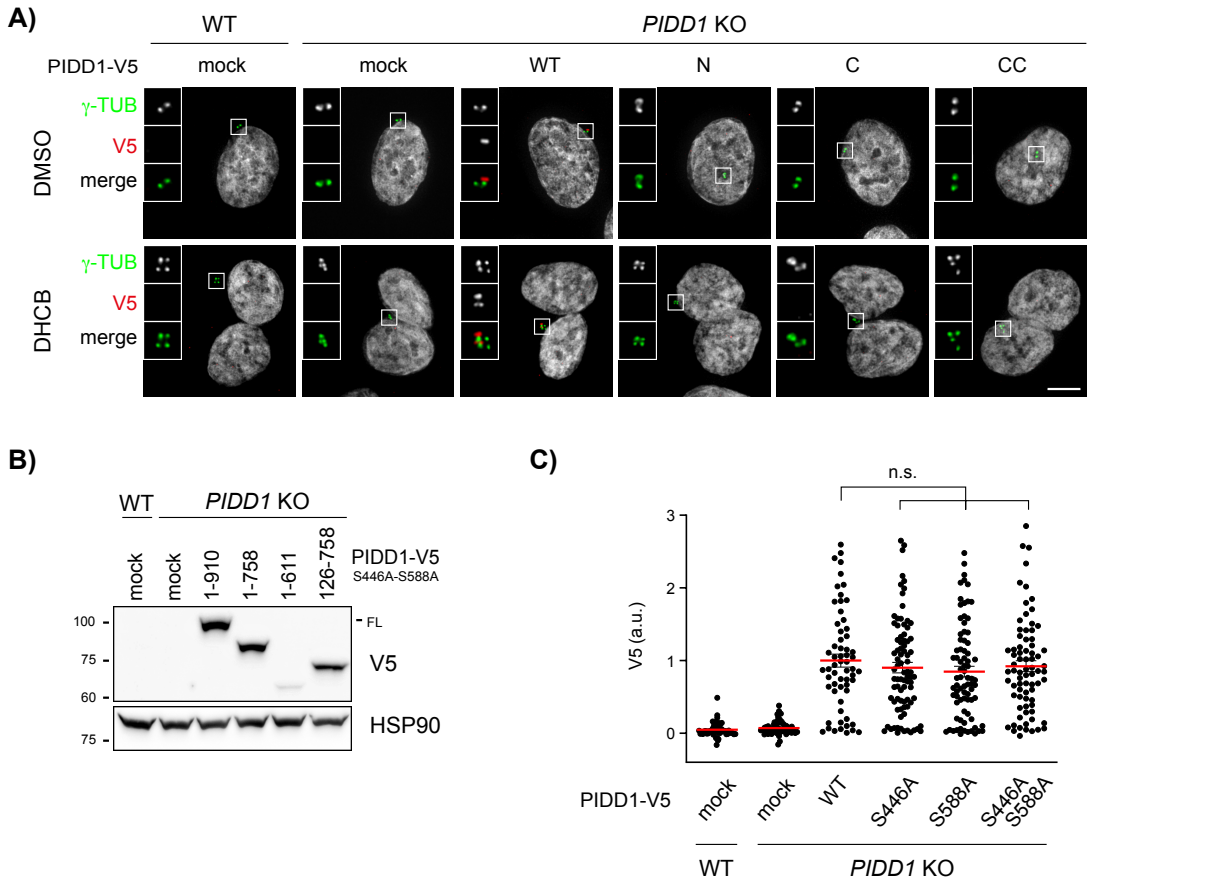

Appendix Figure S4. Data related to Fig. 4 and 5 (A) RPE1 cells of the indicated genotypes were either left untransduced (mock) or transduced with lentiviral vectors expressing PIDD1-V5 in its wild type form or autoprocessing fragments. Cells were treated either with DMSO or with DHCB for 24h and subjected to immunostaining with the indicated antibodies. Blow-ups without Hoechst 33342 are magnified 2.5X. Representative micrographs are shown. Scale bar: 5 μm. **(B)** Immunoblots corresponding to fluorescence micrographs displayed in Fig. 4F. A549 cells of the indicated genotypes were either left untransduced (mock) or transduced with lentiviral vectors expressing the PIDD1-V5 non-cleavable derivative or truncations thereof. N = 2 independent experiments. **(C)** Dot plot showing the average V5 pixel intensities of at individual parent centrioles in A549 cells of the indicated genotypes, either left untransduced (mock) or transduced with lentiviral vectors expressing PIDD1-V5 in its wild type form or carrying the indicated point mutations. N > 50 centrosomes were assessed for each condition in as many individual cells; a.u. = arbitrary units. Kruskal-Wallis test.

A)

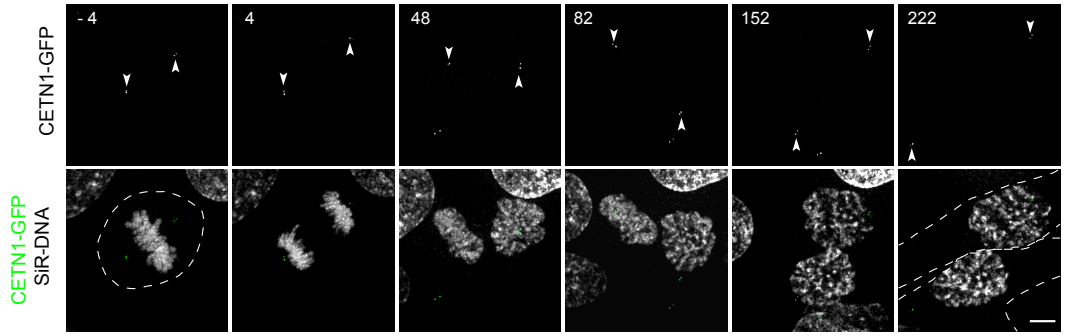

Appendix Figure S5. Untreated control cell related to Fig. 6E (A) Movie stills of a representative RPE1 cell stably expressing CETN1-GFP treated with DMSO, exposed to SiR-DNA and subjected to time-lapse video microscopy. The dashed line indicates the plasma membrane of the cell of interest, arrowheads indicate the centrosome position. Scale bar: 5 µm.

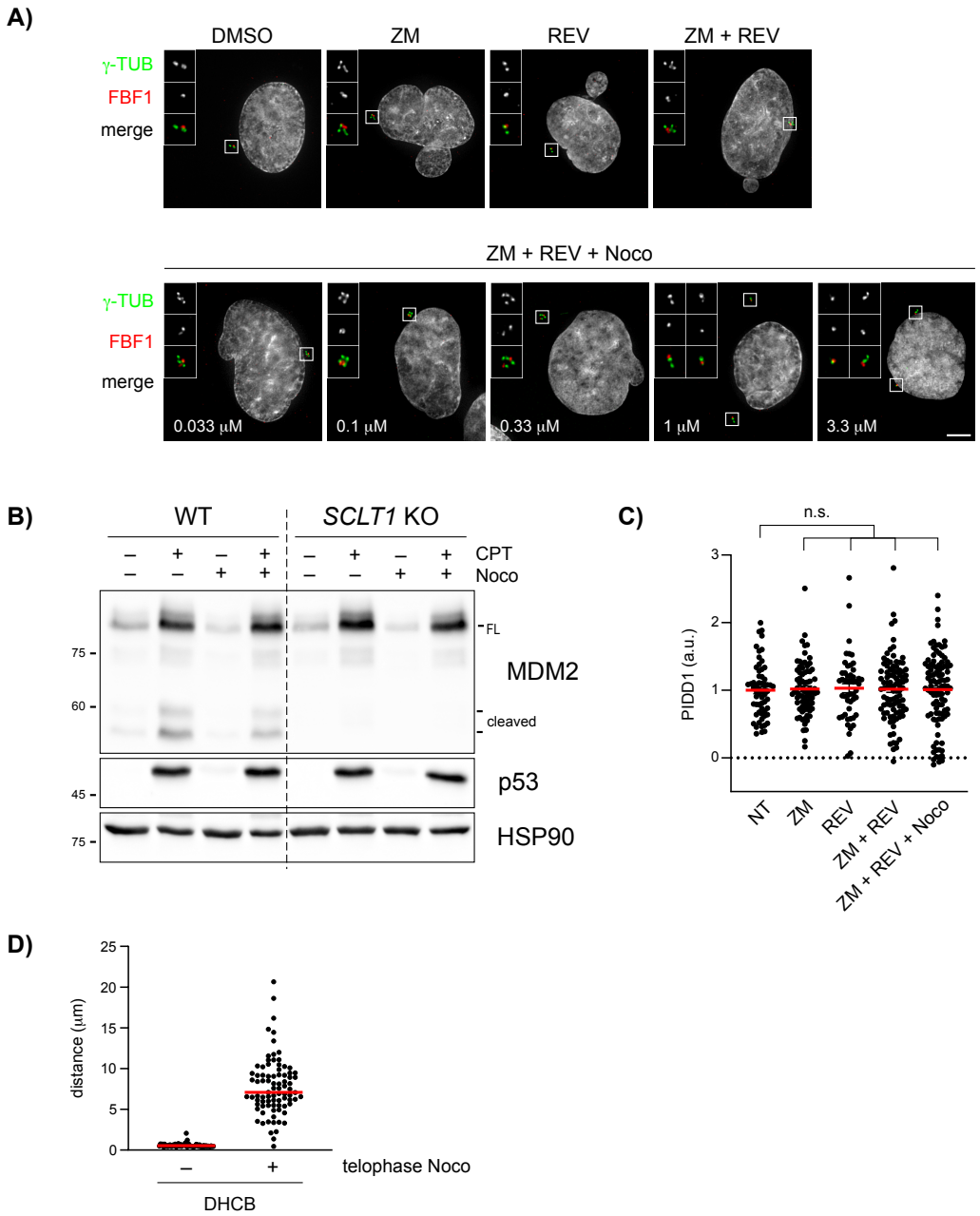

Appendix Figure S6. Data related to Fig. 7. (A) A549 cells were either left untreated (DMSO) or treated with the indicated combination of drugs for 24h and co-stained with the indicated antibodies. Representative fluorescence micrographs are shown. Blow-ups without Hoechst 33342 are magnified 2.5X. Scale bar: 5 μm. **(B)** A549 cells of the indicated genotypes were either left untreated or treated with CPT and/or nocodazole (1 μM) as reported for 24h and subjected to immunoblot. N = 3 independent experiments. **(C)** Dot plot showing the average pixel intensities of PIDD1 at individual parent centrioles in A549 treated as in (A). 1 μM Nocodazole was used. N > 50 centrosomes were assessed for each condition in as many individual cells; a.u. = arbitrary units. Kruskal-Wallis test. **(D)** Distance of parent centrioles in binucleated RPE1 cells subjected to synchronization as in Fig. 7D. Cells were release in DHCB in the absence (-) or presence (+) of nocodazole during telophase. Distances were calculated in ≥ 50 individual cells per condition.

Appendix Methods

Molecular cloning.

Vectors for the generation of CRISPR/Cas9-mediated loss-of-function cell lines were produced using the Lenti-CRISPR-V2 backbone (gift from Feng Zhang; Addgene plasmid #52961). Oligonucleotides yielding small guide RNAs (sgRNAs) targeting the genes of interest were designed using CRISPR Design (http://crispr.mit.edu). LentiCRISPRv2 plasmid was digested with Esp3I (Thermo Scientific #ER0452) and gel purified. Equimolar quantities of complementary oligonucleotides were annealed in 10 mM Tris-HCl pH 7.5, 50 mM NaCl, 1 mM EDTA by heating to 95°C and then slowly ramping down to 25°C. Annealed oligonucleotides were diluted 1:100 in ddH2O and used to set up a ligation reaction with the previously digested backbone, using T4 DNA Ligase (Thermo Scientific #EL0012). All plasmids were verified by Sanger sequencing. A complete list of the sgRNAs used in this work is reported in Table EV2.

Human cDNAs of ANKRD26 (transcript NM_014915) and SCLT1 (transcript NM_144643) were custom synthesized by Eurofins Genomics in the pEX-A258 and pUC57 backbone, respectively. The ANKRD26 synthetic cDNA contained a silent mutation to prevent recognition by sgRNA ANKRD26#2 and ANKRD26#4. pMSCV-Pidd1 T788A (Addgene plasmid #60529) was a gift from Trudy Oliver and Ala788 was backmutated to Thr (obtaining a sequence corresponding to the transcript NM_145886). The desired cDNAs were cloned into pcDNA5/FRT/TO (Invitrogen V652020) in order to generate the following constructs: pcDNA5/FRT/TO-myc-SCLT1, pcDNA5/FRT/TO-myc-ANKRD26 and pcDNA5/FRT/TO-PIDD1-V5. The cDNA of each construct was then subcloned into the lentiviral plasmid FUW-tetO-MCS+ (a modified version of Addgene plasmid #84008, gift by Dr. Alessio Zippo). The PIDD1 construct used for FRAP experiments was built cloning PIDD1^{L828E} cDNA in a FUW-tetO-MCS+ plasmid already containing a mNeonGreen sequence. PIDD1 autoproteolytic fragments, PIDD1 truncating mutations and ANKRD26 mutants were generated by PCR using the primers reported in Table EV2. PCR products were cloned into FUW-tetO-MCS+ plasmid and all constructs were sequence-verified. Site-directed mutagenesis was performed as previously reported (Edelheit *et al*, 2009) with the primers listed in Table EV2. The insertion of the desired mutations was checked by Sanger sequencing.

CRISPR clone characterization.

DNA was extracted from DAP loss-of-function clones using the NucleoSpin Tissue kit (Macherey-Nagel, 740952) following the manufacturer's protocol. For each guide, PCR reactions employing Phusion DNA polymerase (Thermo Scientific, F530-L) were performed, using a primer pair (Table EV2) designed to obtain amplicons spanning the cut site. PCR products were run on an agarose gel and purified using NucleoSpin Gel and PCR Clean-up kit (Macherey-Nagel, 740609), according to manufacturer's instructions. Each amplicon was then sequenced and Inference of CRISPR Edits (ICE) analysis was accomplished thanks to Synthego Bioinformatics tool (https://ice.synthego.com) (Hsiau *et al*, 2018).

Yeast-two-hybrid analyses.

The yeast-two-hybrid screens were performed by Hybrigenics Services, S.A.S., Evry, France. The coding sequence of PIDD1 1-758 S446A/S588A was PCR-amplified and cloned into pB66 as a C-terminal fusion to the Gal4 DNA-binding domain. The construct was used as bait to screen a random-primed Human Lung Cancer Cells cDNA library constructed into pP6. 51 million clones (5-fold the complexity of the library) were screened using a mating approach with YHGX13 (Y187 ade2-101::loxP-kanMX-loxP, matα) and CG1945 (mata) yeast strains as previously described (Fromont-Racine *et al*, 1997). 180 His+ colonies were selected on a medium lacking tryptophan, leucine and histidine. Prey fragments of positive clones were amplified by PCR and sequenced at their 5' and 3' junctions. The resulting sequences were used to identify the corresponding interacting proteins in the GenBank database (NCBI) using a fully automated procedure. For the interaction domain mapping screen, the fragment containing amino acids 538-1204 of ANKRD26 (identified as prey in the previous Y2H screen) was enzymatically fragmented. Fragments were dA-tailed, enriched by PCR and eventually cloned into the yeast prey vector pP9 using homologous recombination in yeast. The ANKRD26 fragment library had a size of 39,000 independent fragments. Amino acids 1-758 of PIDD1 (S446A, S588A) were cloned into pB27 as a C-terminal fusion to LexA (LexA-PIDD1). 1.3 million clones of the ANKRD26 fragment library were screened using a mating approach with YHGX13 (Y187 ade2-101::loxP-kanMX-loxP, matα) and L40DGal4 (mata) yeast strains as previously described (Fromont-Racine *et al*, 1997). His+ colonies were selected on a medium lacking tryptophan, leucine and histidine. Prey fragments of positive clones were amplified by PCR and sequenced at their 5' and 3' junctions. The sequences of 75 experimental ANKRD26 fragments were overlapped and their positions calculated relative to the full-length ANKRD26 protein. The minimal region that overlaps in all experimental ANKRD26 fragments represents the selected interacting domain.

Measurement of centrosomal PIDD1 protein turnover by FRAP.

12,000 PIDD1-deficient RPE1 cells transduced with a lentiviral vector expressing PIDD1-L828E-mNeonGreen were seeded for each well of a 24-well glass bottom dish (Ibidi). Cells were treated with either DMSO or DHCB for 16 hours before imaging on an Axio Observer Z1 microscope (Zeiss) equipped with a 3i Marianas spinning disk confocal system, a CSU-X1 confocal scanner unit (Yokogawa Electric Corporation), Plan-Apochromat 63x/1.4NA Oil Objectives (Zeiss), Orca Flash 4.0 sCMOS Camera (Hamamatsu) and a Vector^{TM} High Speed FRAP module. Imaging was performed in CO_2 independent medium (Gibco, 18045054) supplemented with 10% fetal bovine serum (Clontech), 2 mM L-glutamine (PAN Biotech), 100 IU/mL penicillin, and 100 µg/mL streptomycin (GIBCO). Three independent experiments, for a total of 12 cells, were analysed for both conditions. FRAP analysis was carried out in the presence of either DMSO or DHCB as previously described (Overlack *et al*, 2017). Briefly, a region of interest (ROI) of 1,72 x 1,72 µm containing the centrosomes was bleached for 20 ms with a 488 nm laser line at 100% power. Images were binned 2x2 to increase signal-over-camera noise. At each time point, a z-stack consisting of 3 sections at 0.8 µm intervals was acquired. The mNeonGreen signal was imaged for 4 time-frames before photobleaching. After bleaching, a z-series was acquired every 1 s for a total duration of 2 min with an exposure time of 100 ms. Images were converted into maximal intensity projections and exported as 16-bit TIFF files for measurements of fluorescence intensity recovery rates using ImageJ. Apart from the bleached centrosome, a control non-bleached ROI from the same cell and a non-bleached ROI from outside of the cell (baseline) were also measured. The relative fluorescence intensity was calculated as RFI = $(F_{ROI}(t)/F_{BG}(t)) / (F_{ROI}(t_0)/F_{BG}(t_0))$, as described previously (Chen & Huang, 2001), to correct for background intensity and for photobleaching that occurred during image acquisition. $F_{ROI}(t)$ is the intensity of the bleached ROI containing the centrosome at different time points after bleaching, $F_{BG}(t)$ is the intensity of the control non-bleached ROI at the corresponding time points. $F_{ROI}(t_0)$ is the average intensity of the bleached ROI containing the centrosome for the 4 time-frames before photobleaching, $F_{BG}(t_0)$ is the average intensity of the control non-bleached ROI before bleaching. A baseline value, calculated from the region outside the cell, was subtracted from all values. RFIs were then fitted to a double exponential curve using GraphPad Prism 6.0. Choice of the preferred fitting model was made with an extra sum-of-squares F test (selects the simpler model unless P is <0.05) in which both curves showed a $P<0.0001$.

Quantification of PIDD1 protein species using targeted PRM-LC-MS analysis.

A549 cell samples were resuspended in lysis buffer (0.1 M ammonium bicarbonate, 8 M urea, 5 mM TCEP, and 10 mM chloroacetamide), and lysed with a Bioruptor sonicator (10 cycles,

Bioruptor, Diagnode). Lysates were reduced and alkylated for 1h at 37°C followed by digestion overnight at 37°C with trypsin (1/50 w/w; Promega, Madison, Wisconsin). Peptides were purified using C18 reversed phase spin columns according to the manufacturer's instructions (Macrospin, Harvard Apparatus). Samples were dried under vacuum and stored at -80°C until further use. For targeted MS analysis, proteotypic peptides were selected from public repositories ProteomicsDB (www.proteomicsdb.org) and MaxQB (maxqb.biochem.mpg.de) to represent all PIDD1 fragments with unique and specific sequences. Peptides lacking missed cleavages, methionine and glutamine at the N-termini as well as peptides frequently observed were preferred. The final peptide list is illustrated in Fig. 4E. For these, synthetic heavy reference peptides were ordered (JPT Peptide Technologies) and pooled. In a first step, parallel reaction-monitoring (PRM) assays (Peterson *et al*, 2012) were generated from a mixture containing 100 fmol of each heavy reference peptide and shotgun data-dependent acquisition (DDA) LC-MS/MS analysis on a Thermo Orbitrap Fusion Lumos platform (Thermo Fisher Scientific). The setup of the µRPLC-MS system was as described previously (Ahrné *et al*, 2016). Chromatographic separation of peptides was carried out using an EASY nano-LC 1200 system (Thermo Fisher Scientific), equipped with a heated RP-HPLC column (75 µm x 30 cm) packed in-house with 1.9 µm C18 resin (Reprosil-AQ Pur, Dr. Maisch). Peptides were analysed per LC-MS/MS run using a linear gradient ranging from 95% solvent A (0.1% formic acid) and 5% solvent B (99.9% acetonitrile, 0.1% formic acid) to 45% solvent B over 60 minutes at a flow rate of 200 nl/min. Mass spectrometry analysis was performed on Thermo Orbitrap Fusion Lumos mass spectrometer equipped with a nanoelectrospray ion source (both Thermo Fisher Scientific). Each MS1 scan was followed by high-collision-dissociation (HCD) of the 10 most abundant precursor ions with dynamic exclusion for 20 seconds. Total cycle time was approximately 1 s. For MS1, 1e6 ions were accumulated in the Orbitrap cell over a maximum time of 100 ms and scanned at a resolution of 120,000 FWHM (at 200 m/z). MS2 scans were acquired at a target setting of 1e5 ions, accumulation time of 50 ms and a resolution of 30,000 FWHM (at 200 m/z). Singly charged ions and ions with unassigned charge state were excluded from triggering MS2 events. The normalized collision energy was set to 30%, the mass isolation window was set to 1.4 m/z and one microscan was acquired for each spectrum.

The acquired raw-files were database searched against a human database (Uniprot, download date: 2019/03/27, total of 34350 entries) by the MaxQuant software (Version 1.6.2.3). The search criteria were set as following: full tryptic specificity was required (cleavage after lysine or arginine residues); 3 missed cleavages were allowed; carbamidomethylation (C) was set as fixed modification; Arg10 (R), Lys8 (K) and oxidation (M) as variable modification. The mass tolerance was set to 10 ppm for precursor ions and 0.02 Da for fragment ions. The results were imported to Skyline (version 4.1) by generating a spectral library and manually selecting the peptides of interest and the best 6 transition thereof. Then, a scheduled (10 minute windows) mass isolation lists containing all selected peptide ion masses were exported form Skyline and imported into the Lumos

operating software PRM analysis using the following settings: the resolution of the orbitrap was set to 60k FWHM (at 200 m/z) and the fill time was set to 150 ms to reach a target value of 1e6 ions. Ion isolation window was set to 0.4 Th and the scan range was set to 150-1500 Th. A MS1 scan using the same setting as used for DDA above was included in each MS cycle. Each condition was analysed in biological triplicates. All raw-files were imported into Skyline for protein / peptide quantification. To control for variation in sample amounts, the total ion chromatogram (only comprising peptide ions with two or more charges) of each sample was determined by Progenesis QI (version 2.0, Waters). Here, the best peptide ions peak areas were normalized on total MS1 signal (only considering doubly or higher charged peaks), and relative quantifications were calculated on the mean value of parental non-treated values.

DNA content analysis by flow cytometry.

Cells were harvested, washed with PBS, fixed with ice-cold 70% v/v ethanol in PBS for at least 20 min at -20°C and stored at −20°C until analysis. Fixed cells were centrifuged at 1000 g for 3 min, washed twice with PBS, and stained with 10 µg/mL propidium iodide (Invitrogen, P3566) for 30 min at 37°C in the presence of 100 µg/mL PureLink™ RNase A (Invitrogen, 12091-021). Cells were then analysed in a flow cytometer (FACSCanto, BD Bioscience). Data analysis and figure generation were performed using FlowJo software (FlowJo, LLC).

EdU incorporation assessment by flow cytometry.

DNA replication was assessed via EdU incorporation by pulse labeling asynchronously growing cells. Cells were pulsed for 1h with 10 µM EdU, harvested and prepared for flow cytometry using the Click-iT™ EdU Alexa Fluor® Flow Cytometry Assay kit (Thermo Scientific, C10634), according to the instructions of the manufacturer. Briefly, cells were fixed and permeabilized with the provided solutions. Click-It reaction was performed using an Alexa-647 fluorophore. Eventually, samples were stained with propidium iodide as described above and analysed in a flow cytometer (FACSCanto, BD Bioscience). The percentage of induced tetraploid cells was calculated from values gated as in Appendix Fig. S3 as follows:

$$\%\ of\ cells \geq 4C\ (DHCB) - \%\ of\ cells \geq 4C\ (DMSO)$$

The percentage of proliferating tetraploid cells was calculated as follows:

$$\frac{\%\ of\ cells > 4C\ (release) - \%\ of\ cells\ > 4C\ (DMSO)}{induced\ tetraploid\ cells}$$

Antibodies for immunoblotting.

rat anti-CASP2	(Enzo Life Sciences, ALX-804-356, 1: 1000)
rabbit anti-p53	(Cell Signaling Technology, #9282, 1:1000)
mouse anti-HSP90	(Santa Cruz Biotechnology, sc13119, 1:5000)
mouse anti-MDM2	(Invitrogen, MA1-113, 1:1000)
rabbit anti-CEP83	(Sigma Life Science, HPA038161, 1:500)
rabbit anti-ANKRD26	(GeneTex, GTX128255, 1:500)
mouse anti-myc-tag	(Thermo Fisher Scientific, MA1-980; 1:500)
mouse anti-V5	(Invitrogen, R96025, 1:1000)
mouse anti-CDC27	(BD Biosciences, 610455, 1:1000)
goat anti-rabbit IgG/HRP	(Dako, P0448, 1:5000),
rabbit anti-mouse IgG/HRP	(Dako, P0161, 1:5000),
goat anti-rat IgG/HRP	(Thermo Fisher Scientific, 31470, 1:5000)

Antibodies for immunofluorescence.

Mouse anti γ-tub	(Thermo Fisher Scientific, MA1-19421, 1:1000)
Rabbit anti Odf2	(Sigma Life Science, HPA001874, 1:500)
Rabbit anti Fbf1	(Sigma Life Science, HPA023677, 1:500)
Rabbit anti centrin-1	(Protein Tech, 12794-1-AP; 1:500)
Mouse anti myc-tag	(Thermo Fisher Scientific, MA1-980; 1:500)
Rabbit anti myc-tag	(Cell Signaling Technology, #2278; 1:500)
Mouse anti γ-tub AlexaFluor 488	(SCBT, sc-17787, 1:100)
Mouse anti Cep164	(SCBT, sc-515403, 1:500)
Rabbit anti Cep128	(Sigma Life Science, HPA001116, 1:500)
Mouse anti Arl13B	(SCBT, sc-515784, 1:500)
Mouse anti PIDD1	(Enzo Life Sciences, ALX-804-837, 1:500)
Rabbit anti ANKRD26	(GeneTex, GTX128255, 1:800)
Rabbit anti V5-tag	(Cell Signaling Technology, #13202, 1:500)
Goat anti mouse IgG AlexaFluor488	(Invitrogen, A11029, 1:1000)
Goat anti mouse IgG AlexaFluor 555	(Invitrogen, A21424, 1:1000)
Goat anti rabbit IgG AlexaFluor 488	(Invitrogen, A11034, 1:1000)
Goat anti rabbit IgG AlexaFluor 555	(Invitrogen, A21429, 1:1000)

Goat anti mouse IgG AlexaFluor 647 (Invitrogen, A21236, 1:1000)

For STED imaging, primary antibodies were used at 1:200 dilution and the following secondary antibodies were used:

Goat anti rabbit IgG AlexaFluor 594	(Invitrogen, A11037, 1:120)
goat anti mouse IgG StarRED	(Abberior, 2-0002-011-2, 1:120)
goat anti rabbit IgG STAR 440SXP	(Abberior, 2-0012-003-4, 1:200)
goat anti mouse IgG STAR 488	(Abberior, 2-0002-006-8, 1:200)

Appendix References

Ahrné E, Glatter T, Viganò C, Schubert CV, Nigg EA & Schmidt A (2016) Evaluation and Improvement of Quantification Accuracy in Isobaric Mass Tag-Based Protein Quantification Experiments. *Journal of proteome research* **15:** 2537–2547

Chen D & Huang S (2001) Nucleolar components involved in ribosome biogenesis cycle between the nucleolus and nucleoplasm in interphase cells. *The Journal of cell biology* **153:** 169–176

Edelheit O, Hanukoglu A & Hanukoglu I (2009) Simple and efficient site-directed mutagenesis using two single-primer reactions in parallel to generate mutants for protein structure-function studies. *BMC Biotechnol.* **9:** 61–8

Fromont-Racine M, Rain JC & Legrain P (1997) Toward a functional analysis of the yeast genome through exhaustive two-hybrid screens. *Nature genetics* **16:** 277–282

Hsiau T, Maures T, Waite K, Yang J, Kelso R, Holden K & Stoner R (2018) Inference of CRISPR Edits from Sanger Trace Data. *bioRxiv***:** 251082

Overlack K, Bange T, Weissmann F, Faesen AC, Maffini S, Primorac I, Müller F, Peters J-M & Musacchio A (2017) BubR1 Promotes Bub3-Dependent APC/C Inhibition during Spindle Assembly Checkpoint Signaling. *Current biology : CB* **27:** 2915–2927.e7

Peterson AC, Russell JD, Bailey DJ, Westphall MS & Coon JJ (2012) Parallel reaction monitoring for high resolution and high mass accuracy quantitative, targeted proteomics. *Mol. Cell Proteomics* **11:** 1475–1488